Electrochemical detection of glutathione S-transferase: An important enzyme in the cell protective mechanism against oxidative stress

Manuel C. Martos-Maldonado, Juan M. Casas-Solvas, Antonio Vargas-Berenguel, Luis García-Fuentes*

Department of Chemistry and Physics, University of Almería, Carretera de Sacramento s/n, 04120 Almería, Spain.

*Corresponding author. E-mail: lgarcia@ual.es. Phone: (+34) 950 015618. Fax: (+34) 950 015008.

Running head: Electrochemical detection of glutathione S-transferase

Electrochemical detection of glutathione S-transferase: An important enzyme in the cell protective mechanism against oxidative stress

Manuel C. Martos-Maldonado, Juan M. Casas-Solvas, Antonio Vargas-Berenguel, Luis García-Fuentes

Abstract

Oxidative stress arises when the antioxidant capacity of cells to clean the excess production of reactive oxygen species (ROS) decreases. Several human diseases seem to be related with an increment in the oxidative stress. In this regard, GSH present in the cells works by neutralizing ROS and other xenobiotics through the glutathione S-transferase (GST) enzyme. Thus, the level of expression of GST is an important factor in determining the sensitivity of cells to toxic chemicals or xenobiotic compounds. Therefore, the detection of GST levels is fundamental in the clinical diagnosis of ROS-related diseases. Here, we describe a methodology, based on the voltammetric properties of the ferrocene group (used as electrochemical probe), which can be applied for selective detection of GST levels in human cells. The electrochemical signal measured is associated to the specific interaction of a ferrocenyl-GSH derivate with the G- and H-sites of this enzyme.

Key Words: Ferrocene–glutathione conjugates, Binding, Voltammetry, Electrochemical sensors, Glutathione S-transferase

Running head: Electrochemical detection of glutathione S-transferase

1. Introduction

Xenobiotic compounds of exogenous and endogenous origin are a substantial threat to human cells as they lead to the production of damaging highly reactive oxygen species such as superoxide anions, hydroxyl radicals, and hydrogen peroxide. These reactive oxygen species (ROS) are physiologically produced in the cell through molecular oxygen reduction to water during aerobic metabolism and indiscriminately interact with essential macromolecules such as DNA, proteins and lipids, leading to the disturbance of physiological processes. Thus, excess production or inadequate elimination of ROS lead to increased oxidative stress (OS), which seems linked to the development of some human diseases such as cardiovascular and respiratory diseases, cancer and inflammation-related diseases (1, 2). The glutathione S-transferases (GSTs; EC 2.5.1.18) represent a major group of detoxification enzymes with a broad substrate specificity. All eukaryotic species possess multiple cytosolic and membrane-bound GST isoenzymes, each of which displays distinct catalytic as well as noncatalytic binding properties: the cytosolic enzymes are encoded by at least eight distantly related gene families (named as class alpha, beta, delta, mu, pi, sigma, zeta and theta GST), whereas the membrane-bound enzymes, microsomal GST and leukotriene C_4 synthetase, are encoded by single genes and both have arisen separately from the soluble GST.

Most GSTs exist as dimeric proteins (hetero- and homodimers) of approximately 25 kDa/subunit. Each subunit has an active site composed of two distinct functional regions: a hydrophilic G-site, which binds the physiological substrate glutathione, and an adjacent H-site which provides a hydrophobic environment for the binding of structurally diverse electrophilic substrates (Figure 1) (3). The G-site is highly conserved between all GSTs due to its high specificity for GSH, whereas the H-site can be quite divergent between different GSTs, and exhibits a broad and variable substrate binding specificity. Evidence suggests that the level of expression of GST is a crucial factor in determining the sensitivity of cells to a

broad spectrum of toxic chemicals or xenobiotic compounds. It also appears probable that GST are regulated *in vivo* by reactive oxygen species (ROS), due to the fact that not only are some of the most potent inducers capable of generating free radicals by redox-cycling, but H_2O_2 has been shown to induce GST in plant and mammalian cells. Thus, induction of GST by ROS would appear to represent an adaptive response as these enzymes detoxify some of the toxic carbonyl-, peroxide-, and epoxide-containing metabolites produced within the cell by oxidative stress (3-5). The cells produce numerous antioxidants that counter the effects of these compounds by reducing their accumulation.

Glutathione (GSH) is an important antioxidant that protects against cellular damage caused by environmental toxins as well as from ROS-mediated injury. GSH works by neutralizing ROS and xenobiotics with the help of GST (Figure 2); this enzyme catalyzes the conjugation of GSH to electrophilic substrates, producing compounds that are generally less reactive and more soluble (4). This facilitates their removal from the cell via membrane-based glutathione conjugate pumps. The prevalence of GSTs, together with the evidence suggesting their importance in bioactivation and detoxification of cytotoxic and genotoxic compounds, has stimulated much research into the potential role of these enzymes in diseases. There is also substantial interest in the regulation of cellular GST activity as increased expression of GSTs in tumor cells is frequently associated with multidrug resistance (4, 6). All these properties enhance the importance of these enzymes in the cellular metabolism, which could be used as biomarkers.

Ferrocene (Fc) is a metallocene which has attracted special attention in medicinal research since it is a neutral, chemically stable and nontoxic molecule with excellent voltammetric properties. Fc undergoes a fast and reversible or quasi-reversible one-electron oxidation at potentials which depend on the nature of the substituents attached to the cyclopentadienyl rings. Thus, Fc derivatives have found applications in different areas such

as biosensors, drug research, electrocatalysis and optoelectronics, among others (7). Voltammetric techniques, which are simple, sensitive and suitable for real time monitoring of chemical and biological reactions, cannot be directly used to examine the GST–GSH interactions, due to the fact that GSH does not show discernible voltammetric signals. A frequent approach to study non-electroactive binding pairs by electrochemical methods is to conjugate the ligands with redox label. Following this strategy, we linked a Fc group to GSH. The resulting ferrocene-S-glutathione (GSFc) conjugate (Figure 3) showed good redox properties and turned out to bind the enzyme stronger than native GSH itself (8, 9). The detected electrochemical signal is associated to the specific interaction of GS- and Fc-moieties with the G- and H-sites from the enzyme, respectively. Such features make this GSFc conjugate an excellent candidate to be used as a redox probe for the specific detection of GST.

In this chapter, we describe a methodology for the selective detection of GST by using GSFc conjugate as electrochemical sensor in Differential Pulse Voltammetry (DPV) experiments.

2. Materials

2.1. Equipment

2.1.1. Voltammetric experiments

1. Electrochemical measurements were carried out on a MetrOhm μAutolab III potentiostat connected to an Intel Pentium Dual 2.4 GHz CPU personal computer running Eco Chimie B. V. GPES 4.9 software under Windows XP (*see* Note 1).

2. An electrode tip bearing a 3 mm diameter glassy carbon disc (MetrOhm ref. 6.1204.300) was used as working electrode (*see* Note 2). Such electrode tip was fitted to an electrode shaft (MetrOhm ref. 6.1241.060) through a contact pin M4 / 2 mm (MetrOhm ref. 6.2103.120). This electrode was carefully cleaned prior each measurement as described in Subheading 3.1. Its electrochemical effective area was determined as described in Subheading 3.2.

3. A Radiometer type P101 6×4 mm platinum sheet electrode provided with a 14/12 mm sleeve (MetrOhm ref. 6.1236.020) was used as counter (or auxiliary) electrode (*see* Notes 3-5). This electrode was carefully cleaned prior to each measurement as described in Subheading 3.1.

4. A Ag/AgCl electrode (MetrOhm ref. 6.0724.140) fitted into an electrolyte vessel with 3 mm diameter PTFE capillary and ceramic diaphragm (MetrOhm ref. 6.1240.000) filled with Crison electrolyte solution Crisolyt (3 M KCl) was used as reference electrode (*see* Notes 6,7).

5. Working, counter and reference electrodes were fitted into a 1-50 mL titration vessel (MetrOhm ref. 6.1415.110) equipped with a mounting ring (MetrOhm ref. 6.2036.000), a lid with 5 openings (MetrOhm ref. 6.1414.010) and a gas inlet and overflow tube with valve (MetrOhm ref. 6.1440.010) (*see* Note 8). Titration vessel was placed on a magnetic swing-out stirrer (MetrOhm ref. 2.728.0034) and provided with an 8 mm stirring bar (MetrOhm ref. 6.1903.000).

6. It is advisable to equip the titration vessel with a Faraday cage to prevent and diminish any electromagnetic noise (*see* Note 9).

2.2. Reagents and chemicals

2.2.1. GSFc preparation

1. GSFc conjugate (MW: 505.37 Da) was synthesized from reduced glutathione (GSH) and (hydroxymethyl)ferrocene as published in (9) (*see* Note 10). Reduced GSH, (hydroxymethyl)ferrocene and trifluoroacetic acid were purchased from Sigma-Aldrich and used without further purification.

2. A 500 μM stock solution of GSFc was prepared in 10 mM phosphate buffer, 20 mM NaCl, pH 7.2 (*see* Note 11).

2.2.2. GST enzyme preparation

1. Recombinant glutathione S-transferase (GST) was expressed and purified as reported elsewhere (10) to obtain a solution in 100 mM sodium phosphate, 0.1 mM EDTA, pH 7.0 (*see* Note 12). Protein concentration was measured spectrophotometrically at λ 278 nm using a molar extinction coefficient of 7.01×10^4 M^{-1} cm^{-1} for the dimer. Such solution was divided into 1 mL aliquots and stored as frozen at -80 ºC (*see* Note 13).

2. Several fractions of the purified GST were unfrozen, joined and concentrated to ~150 μM by ultrafiltration in a centriprep-30K device from Millipore (Bedford, USA).

3. The concentrated enzyme was dialyzed twice by using pretreated dialysis membranes Spectra/Por 4 (Spectrum Labs, Inc.) at 4 ºC against 10 mM phosphate buffer, 20 mM NaCl, pH 7.2. Protein concentration of the resulting stock solution was measured as indicated above (*see* Note 11).

4. GST activity was measured on the dialyzed stock solution before using the enzyme in the electrochemical experiments according to Habig & Jakoby (11) (*see* Note 14).

3. Methods

3.1 Working and counter electrodes cleaning processes

This section described a standard protocol to clean working and counter electrodes. This step is pivotal and must be performed prior to each electrochemical experiment. Many substances are able to adsorb on electrodes, especially when glassy carbon electrodes are used as working electrodes. Any traces result in noticeable variations of the electrochemical signal, making measurements irreproducible.

1. Working glassy carbon disc electrode was first immersed in a 0.1 M HNO_3 solution for 5 min at room temperature under stirring and then rinsed with MilliQ water.

2. Working electrode was then polished using a suitable polishing kit (MetrOhm ref. 6.2802.000). Adhesive polishing cloth was stuck in a Petri dish (*see* Note 15) and a small amount of aluminum oxide powder (grain size 0.3 μm) was placed on top and soaked with MilliQ water to form an Al_2O_3-water slurry. The slurry was spread on the polishing cloth and the electrode surface was polished by describing fast ∞-shaped movements for 3 min. The electrode was finally exhaustively rinsed with MilliQ water.

3. Platinum sheet counter electrode was immersed in a 50 % v/v H_2SO_4 solution at room temperature for 5 min under stirring and then rinsed with MilliQ water.

4. Both cleaned working and counter electrodes were finally sonicated in a 1:1:1 H_2O-MeOH-CH_3CN mixture for 5 minutes (*see* Note 16).

3.2. Working Electrode effective area determination

This section describes how to determinate the electrochemical effective area of the glassy carbon disc electrode (12). Effective area of an electrode usually does not match the theoretical area which can be mathematically calculated from its geometry. Thus, the effective area of any new electrode must be determined before the first use as follows. Cyclic voltammetry (CV) experiments are used in this aim (*see* Notes 17,18). Electrodes and vessel must be cleaned before each experiment.

1. A 1 mM $Na_4Fe(CN)_6$ (D_0 = 0.65×10^{-5} cm^2 s^{-1}) solution containing 100 mM KCl as supporting electrolyte (*see* Note 19) was prepared as electroactive probe (*see* Note 11).

2. A 100 mM KCl solution was prepared as blank (*see* Note 11).

3. Blank solution (2.5 mL) was placed in the titration vessel and deoxygenated by bubbling N_2 under stirring for 3 min (*see* Notes 20-22).

4. CV experiments were recorded on the blank solution using -0.5 V as first vertex potential, +0.6 V as second vertex potential and 0.00244 V as step potential. Scan rate (υ) was varied from 0.05 to 0.5 V s^{-1}. Five scans were performed for each scan rate value (*see* Note 23).

5. $Na_4Fe(CN)_6$ solution (2.5 mL) was placed in the clean titration vessel and deoxygenated in the same condition as used for the blank solution.

6. CV experiments were recorded on the $Na_4Fe(CN)_6$ solution using the same parameters described in Subheading 3.2.4. According to Randles-Ševčik equation [1] (*see* Note 17), an increase in the oxidation peak current was observed as υ raised (Figure 4).

7. Subheadings 3.2.5 and 3.2.6. were repeated three times.

8. Blank signals were subtracted from those of $Na_4Fe(CN)_6$ for each υ value.

9. Oxidation peak current (I_{pa}) was measured from the voltammograms for each υ value.

10. Graphical plots of I_{pa} versus $(\upsilon)^{1/2}$ gave a straight line which was fitted to Randles-Ševčik equation [1] (*see* Note 17). Averaged effective area (A) of the electrode was calculated from the slope values obtained from each experiments set.

3.3 Electrochemical detection of GST.

This section describes how to detect GST enzyme using GSFc conjugate as electroactive probe. Differential pulse voltammetry (DPV) experiments are used in this aim (*see* Note 24). The following protocol allows not only the detection of the presence of the enzyme but also the characterization of the interaction process through its binding constant as described in

Subheading 3.3.8. Electrodes and vessel must be exhaustively cleaned before each experiment.

1. A 500 μM GSFc stock solution was prepared in 10 mM phosphate buffer, pH 7.2, containing 20 mM NaCl as supporting electrolyte (*see* Notes 11,19).

2. A ~125 μM GST (concentration given as dimer) stock solution was prepared in the same buffer as described in Subheading 2.2.2. (*see* Notes 11,19).

3. Different amounts of GSFc and GST stock solutions as well as pure buffer were mixed to prepare six 2.5 mL samples containing 50 μM GSFc and increasing amounts of GST (from 0 to 90 μM). More concentrated GST samples might be needed depending on the GST source. Each sample was prepared prior to use mixing the stock solutions directly in the clean titration vessel.

4. Each sample solution was deoxygenated by bubbling N_2 under stirring for 3 min (*see* Notes 20-22).

5. A DPV experiment was recorded on each sample solution using -0.2 V as initial potential (E_i), +0.6 V as final potential (E_f), 0.02 V as step potential (ΔE_s), 0.05 V as modulation amplitude (ΔE_p), 2 s as interval time (τ) and 0.05 s as modulation time (t_p), which results in a scan rate (υ) of 0.01 V s^{-1} (*see* Note 24).

6. DPV voltammograms displayed a progressive decrease of the peak current intensity as the GST concentration increased (Figure 5), indicating the binding interaction between the electroactive probe GSFc and the enzyme.

7. Oxidation peak current (I_p) was measured from the DPV voltammograms for each sample and plotted versus GST concentration to yield a non-linear calibration curve for the detection of GST enzyme (Figure 5) (*see* Note 25).

8. I_p data were fitted to a suitable binding model in order to estimate the corresponding binding constant K (*see* Note 26).

9. In order to estimate the limit of detection (LOD) for GST, first linear section of data were also fitted to a line (Figure 5). LOD was defined as the lowest enzyme concentration which gives a signal variation on the oxidation peak equivalent to three times the standard deviation of the peak current measured for the solution of 50 μM GSFc in the absence of enzyme, that is, LOD = $3\sigma/b$; where σ is the standard deviation of the electrochemical signal for that solution (from 3 measurements) and b is the slope of the linear fitting (13).

4. Notes

1. MetrOhm μAutolab III is the most basic and affordable instrument in Autolab family, but can be used for most electrochemical techniques. Eco Chimie B. V. GPES software has recently been discontinued and replaced by the new data acquisition and analysis software package NOVA, for which the following PC configuration is recommended according with the manufacturer: Processor 2 GHz or higher, 80 Gb HDD, 2 Gb RAM, USB port, Windows XP, Vista, Windows 7 or Windows 8 (32 bit).

2. The intensity of the signal is directly proportional to the working electrode surface (14-16), and thus large working electrodes would be desirable in order to increase the sensitivity of the technique. However, it is advised to use counter electrodes larger than working ones (*see* Note 5), which in practice limits the size of the working electrodes that can be used. Signal intensity also increases with increasing modulation amplitude (ΔE_p) (*see* Note 24), but larger amplitudes will also broaden the peak, lowering potential resolution. Moreover, the peaks can be distorted due to non-linearity effects at larger amplitudes. Thus, ΔE_p value must be balanced for each particular case.

3. This electrode is no longer commercialized. Current alternative is Radiometer M241PT platinum plate electrode. Radiometer electrodes are thinner than other trademarks (7.5 mm *versus* 12 mm) and thus fit better in small titration vessels such as that used in this protocol

(It has to be taken into account that three electrodes and a gas inlet tube must be immersed in 2.5 mL of sample solution). However, this feature makes the electrode unable to fit in the MetrOhm sleeve. The sleeve must be attached to the electrode at a suitable position in order to ensure electrode immersion is repeatable in each experiment.

4. Any convenient electrode can be used as the counter one, since its nature should have little to no effect on the electroanalytical measurement. However, it is advisable to choose inert electrodes which do not undergo electrolysis processes that would produce substances that may cause interfering reactions on the working electrode surface.

5. Many electrochemical texts recommend using a counter electrode "much larger" (*sic*) than the working electrode, so that its capacitance handles most of the current required at the reference/counter terminus (14-16). In other words, the half-reaction occurring at the auxiliary electrode must occur fast enough so as not to limit the process at the working electrode. If this does not happen, inaccuracies may arise due to the additional resistance imposed by the counter electrode, which causes an increase of the uncompensated ohmic potential drop at the working electrode. This effect may be significantly large when resistive nonaqueous media are used, but it is less important in experiments carried out in water. In addition, for most of the techniques this phenomena can be extensively diminished in a number of ways where using a "much larger" counter electrode is not compulsory, such as setting a suitable placement for the electrodes (*see* Note 8) and using a high-enough concentration of supporting electrolyte (*see* Note 19). However, it is recommendable to employ a counter electrode reasonably bigger than the working one.

6. No bubbles must be present in the capillary tube. A Pasteur pipette should be used to fill it. Electrolyte vessel must be filled up to ensure reference electrode bulb is completely immersed in the electrolyte solution. Electrolyte level must be periodically checked and renewed.

7. When reference pack (reference electrode + electrolyte vessel) is not going to be used for a short period of time, it should be placed in a suitable beaker filled with some electrolyte solution in order to keep ceramic diaphragm and inner electrolyte solution in good conditions.

8. In order to compensate a major fraction of the cell resistance, the reference electrode should be placed as close as possible to the working electrode (14-16). All measurements must be carried out with the same electrodes placement and orientation.

9. External sources such as computer monitors, other instruments or power lines generates electromagnetic fields able to interfere with the electrochemical setup, causing serious instabilities which can easily be identified due to the appearance of saw-toothed lines in the voltammograms. Commercial Faraday cages are available from a number of sources. However, a simple Faraday cage can be built by covering the titration vessel with aluminum foil connected to the grounding cable provided by the potentiostat.

10. Briefly, a solution of reduced glutathione (50 mg, 0.163 mmol) in water (2 mL) and trifluoroacetic acid (40 μL, 0.489 mmol) were added to a solution of (hydroxymethyl)ferrocene (53 mg, 0.245 mmol) in ethanol (2 mL). An excess of (hydroxymethyl)ferrocene was used in order to ensure the complete consumption of GSH and, hence, simplify the subsequent purification step. The mixture was stirred at room temperature until GSH was no longer observed by TLC (*ca.* 2.5 h). To follow the reaction by TLC (Merck Silica Gel 60 F_{254} aluminum sheets) it is advisable to use CH_3CN/H_2O 3:1 as eluent, where GSH exhibits $R_f = 0.3$. UV light and ethanolic sulfuric acid (5% v/v) were used to develop TLC plates. pH was then increased to 9-10 by dropping a saturated $NaHCO_3$ aqueous solution, and the solvent was removed by rotary evaporation under vacuum. Evaporation temperature was kept below 75 ºC. GSFc conjugate was finally isolated from the crude by column chromatography on silica gel using CH_3CN/H_2O 5:1 as a yellow powder (86

mg, 96 %). Our experience suggests that silica gel 230-400 mesh, ASTM from Merck gives the best results in columns that use aqueous mixtures as eluents.

11. All stock solutions were always freshly prepared prior experiments using MilliQ water (18.2 MΩcm). Stock solutions were disposed of after experiments.

12. Pure GST is also available from a number of commercial sources.

13. Purified enzyme is stable in these conditions for 3-4 months.

14. Briefly, the conjugation reaction (GSH–CDNB) was continuously recorded spectrophotometrically at λ 340 nm ($\varepsilon = 9600\ M^{-1}\ cm^{-1}$) and 25 ºC for 2 min on a Cary BIO 50 spectrophotometer (Varian). For the activity assay, a reaction mixture consisting in 1.5 μM GST, 1 mM GSH and 1 mM 1-chloro-2,4-dinitrobenzene (CDNB) buffered solution (final volume: 1 mL) was prepared by adding solutions of such reagents to a 0.1 M potassium phosphate buffer, pH 6.5. GST was added as an aliquot (10-20 μL) from the stock solution; volume being dependent on the concentration of that solution. GSH was added as 10 mM solution in 0.1 M potassium phosphate buffer, pH 6.5 (100 μL). CDNB was added as a freshly prepared, light-protected 20 mM ethanolic solution (50 μL). It is assumed that the small volumes of GST and CDNB added have a negligible effect on the buffer of the reaction mixture. CDNB solution must be added the last as it marks the initiation of the reaction. One unit of GST activity was defined as the conjugation of 1 μmol of CDNB with GSH per minute at 25 °C. All GST activity assays were performed in conditions of linearity with respect to incubation time and protein concentration. Initial rate of product formed was determined from slope of the increase in absorbance per minute at λ 340 nm. These rates measured as absorbance/time were converted in concentration/time using the indicated molar absorptivity. Determined activity units were compared with the valid range for each GST source. Some commercial kits and explicative protocols for GST activity assays can also be found in the literature.

15. Petri dish provides a convenient container for the polishing cloth. It is cheap, flat, stable, easy-to-grab and easy-to-store. Once used, aluminum oxide is wasted and the polishing cloth can be stored in the Petri dish until the next use.

16. MilliQ water and HPLC grade MeOH and CH_3CN were used. A beaker was filled up with the mixture and placed in the sonicator. The mixture may warm up during sonication. This does not affect the electrodes.

17. Briefly, cyclic voltammetry (CV) is a potential sweep method where potential is linearly varied forwards and backwards between two values (vertex potentials) with time, yielding a triangular potential waveform which causes the oxidation and subsequent reduction of the electroactive species (14-16). The slope of the potential variation defines how fast the experiment is and is called scan rate (υ, V s^{-1}). Usually, this potential profile is repeated a number of cycles in order to reach a stationary state. Measurement of the resulting current at the working electrode during the potential scans gives a cyclic voltammogram where two curves are observed for a reversible system defined by their corresponding oxidation (or anodic) and reduction (or cathodic) peaks (Figure 6). Each peak provides two observable, the peak potentials (E_{pa} and E_{pc} in Volts, respectively), which allow estimating the reversibility as well as formal and half-wave potentials of the system, and the peak currents (I_{pa} and I_{pc} in Ampers, respectively). For a reversible couple, the peak current is given by the Randles-Ševčik equation:

$$I_p = 0.4463 \left(\frac{F^3}{RT}\right)^{1/2} n^{3/2} A C^* \sqrt{\upsilon D_0} \quad [1]$$

where F is the Faraday constant (9.64853×10^4 C mol^{-1}), R is the molar gas constant (8.31447 J mol^{-1} K^{-1}), T is temperature (K), n is the number of exchanged electrons, A is electrode area (cm^2), C^* is bulk concentration of the electroactive species (mol cm^{-3}), υ is the scan rate (V s^{-1}) and D_0 is the diffusion coefficient (cm^2 s^{-1}).

18. According to equation [1] (*see* Note 17), electrode area (A) can be calculated by measuring the peak current (I_p) at different scan rates (υ) for a redox species the diffusion coefficient of which (D_0) is known.

19. Mathematical treatment for most electrochemical methods is based on the assumption that mass transport in solution is affected by a single mechanism, typically diffusion. Thus, other mass transport mechanisms such as convection and migration must be avoided. For convection suppression, sample solution must be kept completely quiet during measurement. Migration, which is the movement of ions under the influence of an electric field, is overcome by adding a large excess of an easily ionizable salt which will dissociate into inert ions and cations. These ions will be the major species affected by migration, releasing the species of interest from that effect. Such salt is called supporting electrolyte, and is must be about 100 times more concentrated that the analyte.

20. Oxygen is a redox species able to generate residual faradaic currents under certain conditions, and thus any electrochemical experiment must be performed in degassed solutions.

21. N_2 must be softly bubbled and stirring must be gentle in order to minimize foam formation, especially when any protein is present in the solution.

22. To avoid any convection effect, an equilibration time of at least 20 s should be applied after N_2 bubbling before starting measurement.

23. The characteristic peaks in a cyclic voltammogram are caused by the formation of a diffusion layer near the electrode surface which requires more than one scan to reach a stationary state. This can be seen simply comparing the voltammograms obtained after each cycle, as usually an increase in the peak currents can be observed. Strictly speaking, one should wait for the peak current to remain unchanged, but our experience suggests that after

five scans peak current variations are negligible. Data must always be extracted from the last scan.

24. Briefly, differential pulse voltammetry (DPV) is a pulsed voltammetric technique where potential excitation functions are more complicated than that showed by CV (*see* Note 17). However, they yield much higher sensitivities (~10^{-8} M) than potential sweep methods as CV (~10^{-4} M) and thus are more adequate for analytical measurements (14-16). DPV waveform is composed of a series of potential pulses where current is measured at two different times per pulse, before and at the end of the pulse (Figure 7). The quantity of interest in DPV is the difference between those two values. Four parameters are needed to completely define the DPV waveform: step potential (ΔE_s), modulation amplitude (ΔE_p), interval time (τ) and modulation time (t_p). Step potential and interval time defines the scan rate (υ) as $\Delta E_s/\tau$. In addition, initial and final potentials have also to be set up. Resulting voltammograms consist of a single current peak per redox process, the height of which is directly proportional to the concentration of the corresponding electroactive species.

25. The method has a narrow linear dynamic range and should be used only as a qualitative analysis to detect the presence of GST.

26. Taking into account GST is a dimer (Figure 2), a two equal and independent sites model was used to fit the DPV voltammetric data obtained from GSFc oxidation. The binding parameter (ν), defined as the ratio between the concentrations of bound ligand ($[L]_b$) and the total macromolecule ($[M]_t$), is expressed as:

$$\nu = \frac{[L]_b}{[M]_t} = \frac{2K[L]}{1 + K[L]} \quad [2]$$

where K and [L] are the equilibrium association constant and the free ligand concentration, respectively. The latter is related to the total ligand ($[L]_t$) and the bound ligand ($[L]_b$) by the mass conservation law:

$$[L] = [L]_t - [L]_b \quad [3]$$

Under the assumptions of a reversible, diffusion-controlled electron transfer and a diffusion coefficient for the bound ligand much lower than that for the free ligand, the following approximation can be made:

$$\frac{[L]}{[L]_t} = \frac{I_p}{I_{p,0}} \quad [4]$$

Where I_p and $I_{p,0}$ are the peak current in the presence and in the absence of protein, respectively. An algorithm including equations [2]-[4] was compiled using Scientist software (Micromath Scientific Software, St. Louis, USA) to fit the experimental data.

Acknowledgments

The authors acknowledge financial support from the Spanish Ministry of Economy and Competitiveness and the EU European Regional Development Fund (Grant CTQ 2010-17848), as well as the Andalusian Regional Government (Consejería de Economía, Innovación y Ciencia, Junta de Andalucía, grants CVI-6028 and FQM-6903).

References

1. Valko M., Leibfritz D., Moncol J., Cronin M.T., Mazur M., Telser F. (2007) Free radicals and antioxidants in normal physiological functions and human disease. *Int J Biochem Cel Biol* **39**: 44-84.
2. Quaye I.K. (2012) Oxidative stress in human health and disease. In: Priti R (ed) Insight and control of infectious diseases in global scenario, InTech, Rijeka, Croatia, pp 97-120.
3. Hayes J.D., Flanagan J.U., Jowsey I.R. (2005) Glutathione transferases, *Annu Rev Pharmacol Toxicol* **45**: 51-88.
4. Eaton D.L., Bammler T.K. (1999) Concise review of the glutathione S-transferases and their significance to toxicology. Toxicol Sci **49**: 156-64.

5. Hayes J.D., McLellan L.I. (1999) Glutathione and Glutathione-dependent enzymes represent a co-ordinately regulated defence against oxidative stress. *Free Rad Biol Med Res* **31**: 273-300.
6. Laborde E. (2010) Glutathione transferases as mediators of signaling pathways involved in cell proliferation and cell death. *Cell Death Differ* **17**: 1373–1380.
7. Fouda M.F.R., Abd-Elzaher M.M., Abdelsamaia R.A., Labib A.A. (2007) On the medicinal chemistry of ferrocene. *Appl Organomet Chem* **21**: 613–625.
8. Martos-Maldonado M.C., Quesada-Soriano I., García-Maroto F., Vargas-Berenguel A., García-Fuentes L. (2012) Ferrocene labelings as inhibitors and dual electrochemical sensors of human glutathione S-transferase P1-1. *Bioorg Med Chem Lett* **22**: 7256-7260.
9. Martos-Maldonado M.C., Casas-Solvas J.M., Téllez-Sanz R., Mesa-Valle C., Quesada-Soriano I., García-Maroto F., Vargas-Berenguel A., García-Fuentes L. (2012) Binding properties of ferrocene-glutathione conjugates as inhibitors and sensors for glutathione S-transferases. *Biochimie* **94**: 541-550
10. Yassin Z., Ortiz-Salmerón E., García-Maroto F., Barón C., García-Fuentes L. (2004) Implications of the ligandin binding site on the binding of non-substrate ligands to *Schistosoma japonicum*-glutathione transferase, *Biochim Biophys Acta* **1698**: 227-237.
11. Habig W.H., Jakoby W.B. (1981) Assays for differentiation of glutathione S-transferases, *Methods Enzymol* **77**: 398-405.
12. Casas-Solvas J.M., Ortiz-Salmerón, E., Giménez-Martínez J.J., García-Fuentes L., Capitán-Vallvey L.F., Santoyo-González F., Vargas-Berenguel A. (2009) Ferrocene-carbohydrate conjugates as electrochemical probes for molecular recognition studies, *Chem Eur J* ***15***: 710-725.

13. MacDougall D., Crummett W.B. (1980) Guidelines for data acquisition and data quality evaluation in environmental Chemistry, *Anal Chem* **52**: 2242-2249.
14. Bard A.J., Faulkner, L.R. (2001) Electrochemical Methods. Fundamentals and Applications, 2nd Edition. John Wiley & Sons, Inc., New York. Sections 6.1, 7.3.4, and 15.6.
15. Wang J. (2001) Analytical Electrochemistry, 2nd Edition. John Wiley & sons, Inc., New York. Sections 2-1, 3-3.2 and 4-4.
16. Kaifer A.E., Gómez-Kaifer M. (1999) Supramolecular Electrochemistry. Wiley-VCH Verlag GmbH, Weinheim. Sections 1.2, 4.2 and 4.3.

Figure captions

Figure 1. Overview of homodimeric structure of human GST P1-1 from PDB entry 11GS. The subunits are shown as surfaces. The functional active site in a subunit (G- and H-site) has been enlarged for easy viewing.

Figure 2. Co-ordinate interaction between cellular GSH, glutathione S-transferase (GST) and glutathione S-conjugate efflux pump MRP. ROS, reactive oxigen species; GSSG, oxidized glutathione; GPX, glutathione peroxidase; GR, glutathione reductase; GS-X, glutathione conjugate of X; MRP, multidrug resistance associated protein.

Figure 3. Ferrocene-S-glutathione (GSFc) conjugate chemical structure.

Figure 4. a) Partial cyclic voltammograms (5 scans) measured between -0.5 V and +0.6 V for 1 mM $Na_4Fe(CN)_6$ solution containing 100 mM KCl as supporting electrolyte after subtracting blank (100 mM KCl) signal at increasing scan rates (υ) from 0.05 to 0.5 V s^{-1}. An increase in the peak currents (large arrow) was observed as υ raised (small arrow). b) Oxidation peak current (I_{pa}) data plotted versus $\upsilon^{1/2}$. Solid line: Data were fitted to Randles-Ševčik equation [1] (*see* Note 17) in order to estimate effective area (A) of the working glassy carbon disc (3 mm diameter) electrode (A = 0.038±0.006 cm^2 in average after three measurements).

Figure 5. a) DPV curves for 50 μM GSFc in the presence of increasing amounts of *Schistosoma japonica* glutatione S-transferase (SjGST) ranging from 0 to 90 μM in 10 mM phosphate buffer, pH 7.2, containing 20 mM NaCl as supporting electrolyte. Following parameters were used: -0.2 V as initial potential (E_i), +0.6 V as final potential (E_f), 0.02 V as step potential (ΔE_s), 0.05 V as modulation amplitude (ΔE_p), 2 s as interval time (τ) and 0.05 s as modulation time (t_p), which resulted in a scan rate (υ) of 0.01 V s^{-1}. A decrease in the current intensity (large arrow) was observed as SjGST concentration increased (small arrow). b) Peak current intensity (DPV) variation for GSFc oxidation versus SjGST concentration. Solid line: Data were fitted to a two equal and independent sites model (*see* Note 26) in order to estimate binding constant value (K = (2.1±0.9)×10^4 M^{-1}). Dashed line: The first linear section of the data was fitted to a line in order to estimate limit of detection as described in Subheading 3.3.9 (LOD = 11 μM).

Figure 6. a) CV waveform for the oxidation of an electroactive species, where E_{v1} and E_{v2} are the vertex potential and υ (the slope of the line) is the scan rate. b) Partial cyclic voltammogram for the oxidation of an electroactive species, where E_{pa} and E_{pc} are the anodic

and cathodic peak potentials, respectively, and I_{pa} and I_{pc} are the anodic and cathodic the peak currents, respectively.

Figure 7. a) DPV waveform for the oxidation of an electroactive species, where ΔE_s is the step potential, ΔE_p is the modulation amplitude, τ is the interval time and t_p is the modulation time. Such waveform is applied between initial (E_i) and final (E_f) potentials. Scan rate (υ) in DPV is defined the as $\Delta E_s/\tau$. b) DPV voltammogram for the oxidation of an electroactive species, where E_p and I_p are peak potential and peak current, respectively.

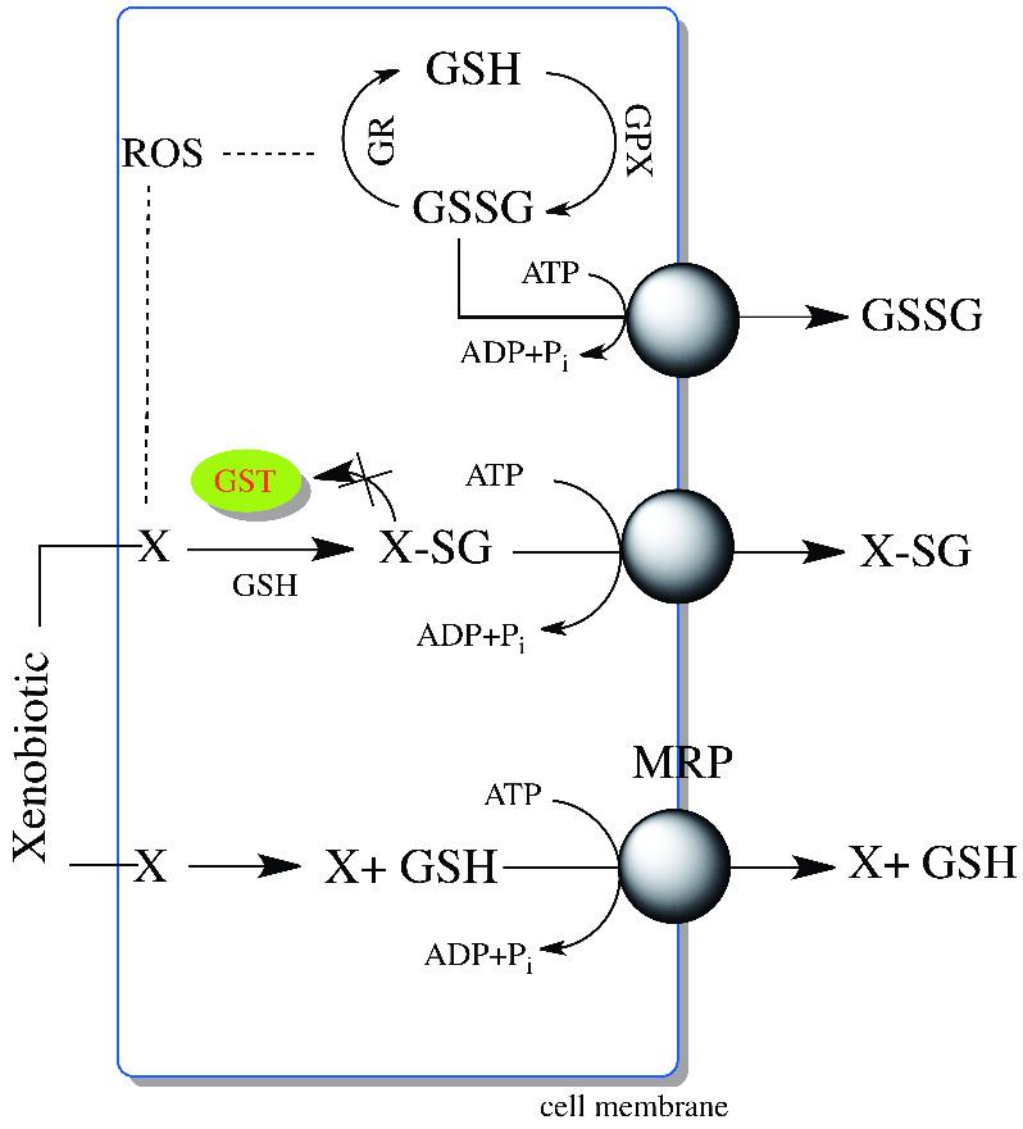
GSH
GR
GPX
ROS
GSSG
ATP
ADP+P$_i$
GSSG
GST
ATP
X
X-SG
X-SG
GSH
ADP+P$_i$
Xenobiotic
MRP
ATP
X
X+ GSH
X+ GSH
ADP+P$_i$
cell membrane

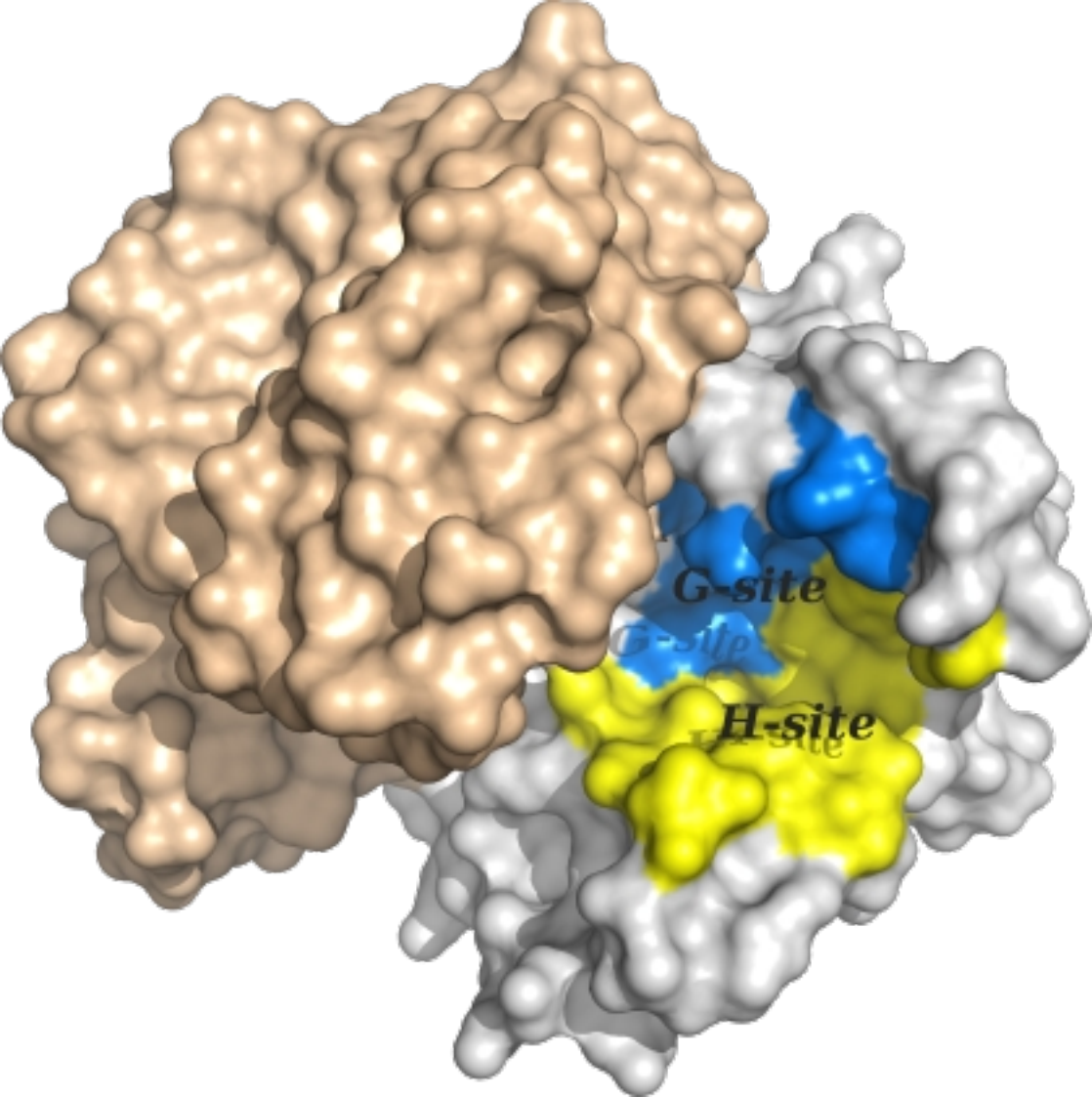
G-site
H-site

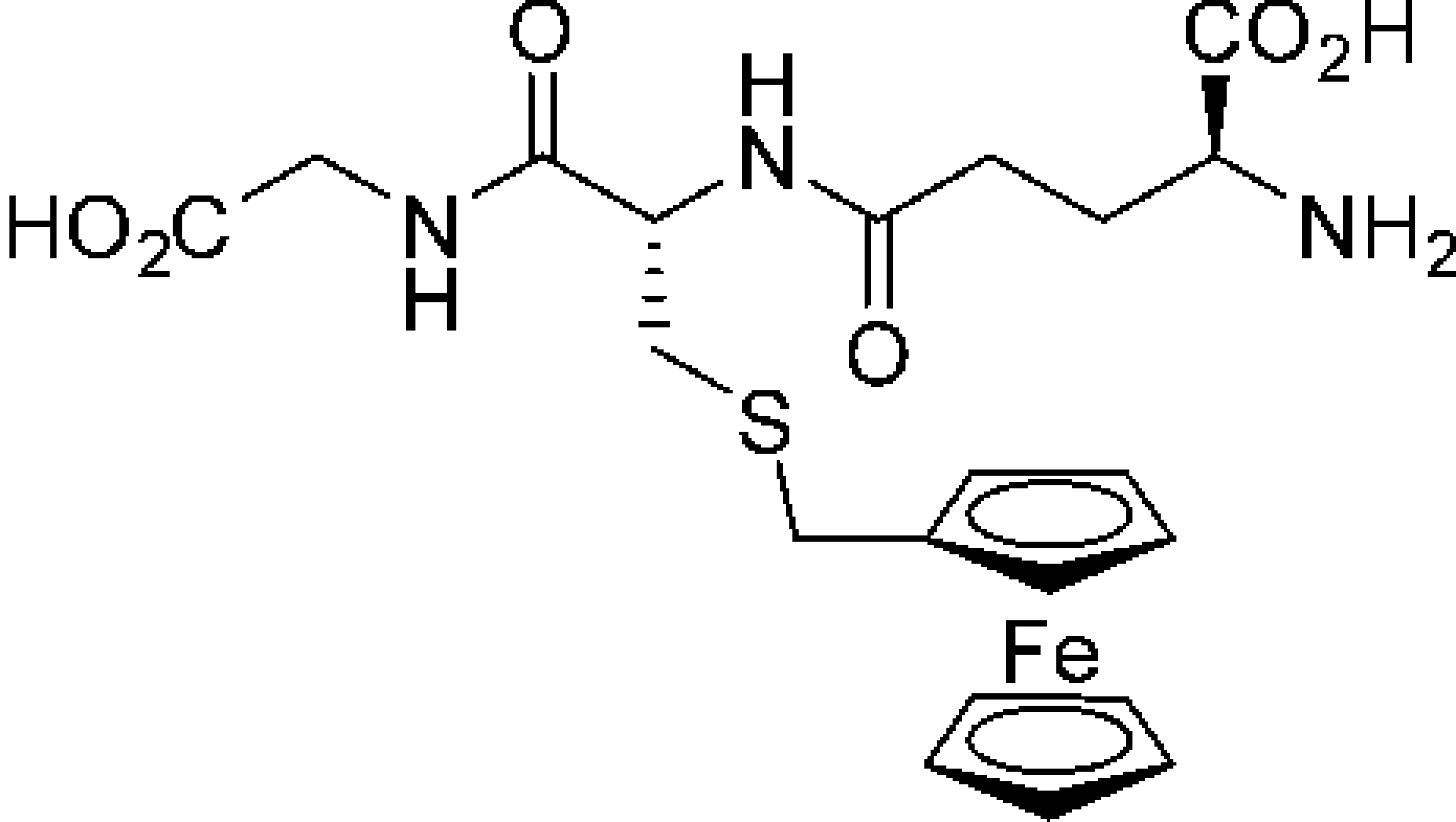
HO2C
N
H
O
H
N
O
S
CO2H
NH2
Fe

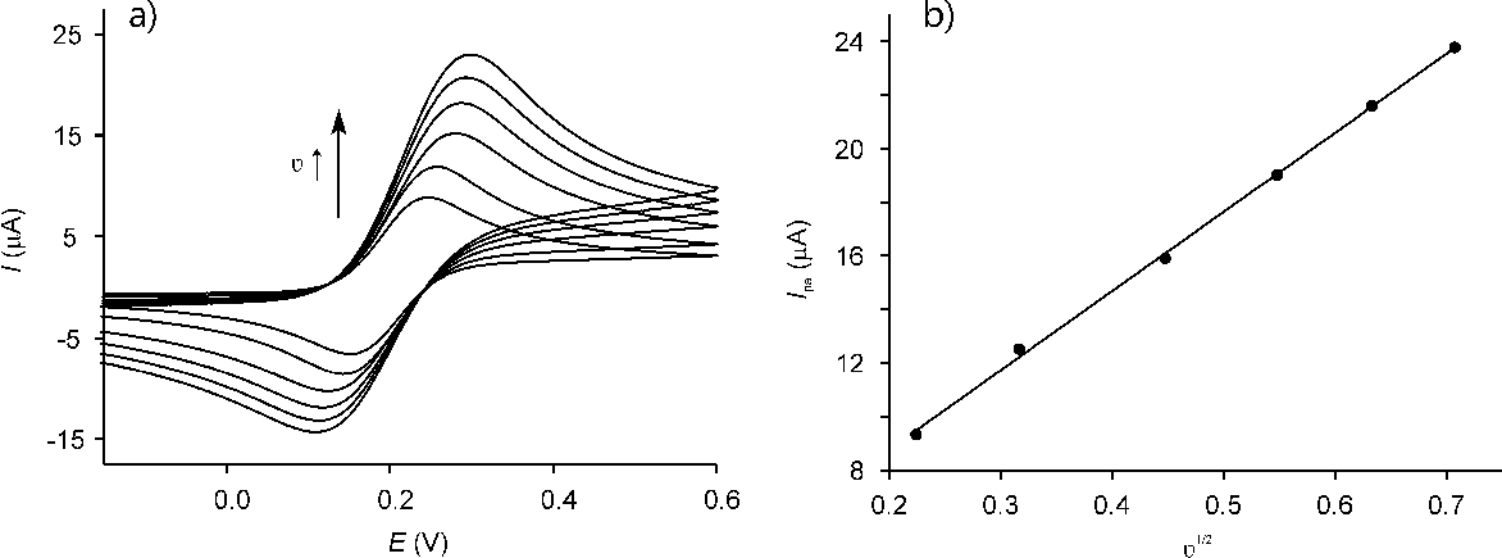
a)
25
15
5
-5
-15
I (μA)
υ
0.0
0.2
0.4
0.6
E (V)
b)
24
20
16
12
8
I_{pa} (μA)
0.2
0.3
0.4
0.5
0.6
0.7
$υ^{1/2}$

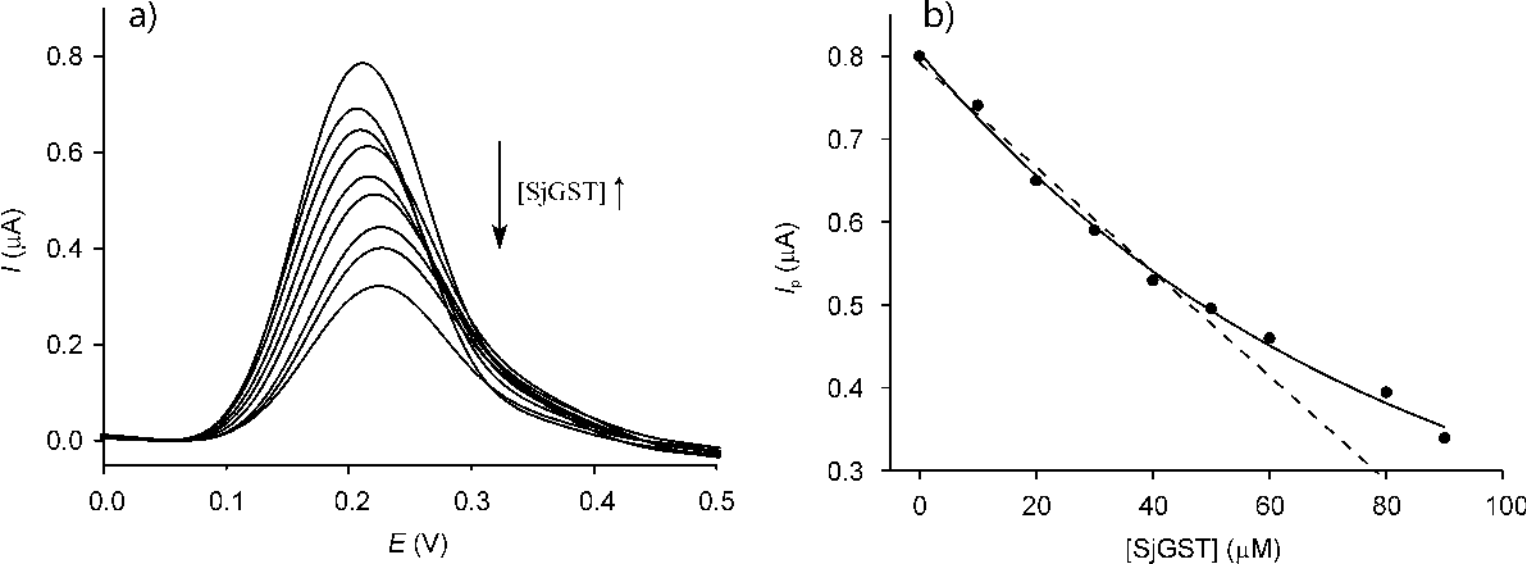
a)
0.8
0.6
0.4
0.2
0.0
I (μA)
[SjGST] ↑
0.0
0.1
0.2
0.3
0.4
0.5
E (V)
b)
0.8
0.7
0.6
0.5
0.4
0.3
I_p (μA)
0
20
40
60
80
100
[SjGST] (μM)

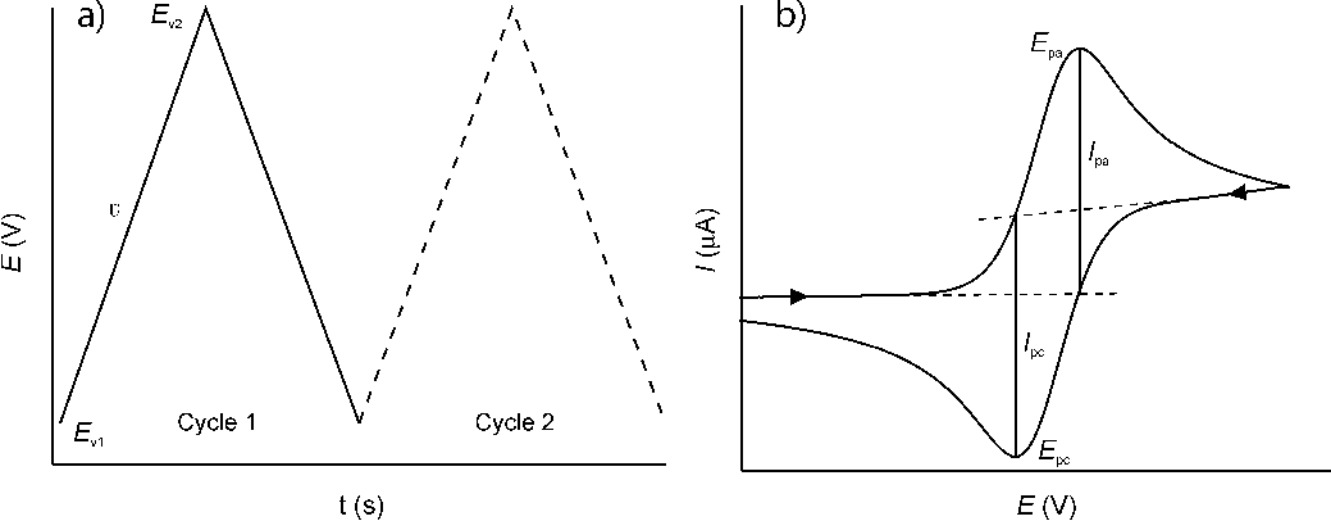
a)
E_{v2}
E_{v1}
Cycle 1
Cycle 2
E (V)
t (s)
b)
E_{pa}
I_{pa}
I_{pc}
E_{pc}
I (μA)
E (V)

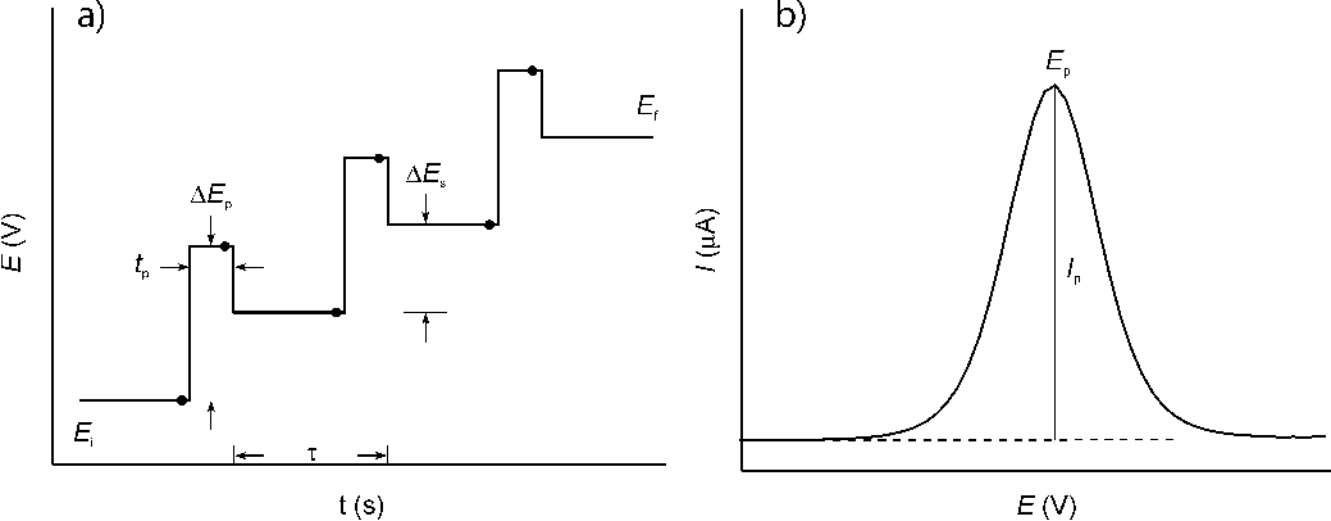
a)
E (V)
t (s)
E_f
E_i
ΔE_p
ΔE_s
t_p
τ
b)
I (μA)
E (V)
E_p
I_p